CLOUD-TOP HEIGHT ESTIMATION FROM SATELLITE STEREOPAIRS FOR WEATHER FORECASTING AND CLIMATE CHANGE ANALYSIS

Daniela POLI, Gabriela SEIZ, Manos BALTSAVIAS
Federal Institute of Technology, Zurich
Institute of Geodesy and Photogrammetry
(daniela, gseiz, manos)@geod.baug.ethz.ch

KEYWORDS: Climate Change, Image Matching, Cloud Top Heights, MOMS, ATSR.

ABSTRACT

Within the EU project Cloudmap, cloud-top heights should be estimated using satellite stereo images at very high temporal resolution. Since such images are not provided by operational sensors, MOMS-2P and ATSR2 images of lower temporal resolution were used instead. The MOMS stereopair was oriented with subpixel accuracy using GCPs from 1:50,000 topographic maps and Kratky's sensor model. Preprocessing for noise reduction, cloud stripes removal and contrast enhancement was applied. For the estimation of cloud-top heights, the images were resampled to 288 m and geometrically constrained least squares matching, using image pyramids and an interest operator, as well as varying parameters was used. The results were checked by visual inspection and comparison to semi-automatically measured points in the original resolution images. Automatic blunder detection using two tests were also applied. Matching led to large blunders in land areas between clouds or close to cloud boundaries. Excluding these blunders (error > 1100 m), matching showed an RMS of ca. 0.2 pixel, exhibiting a very high accuracy potential. A matching geometric transformation using rotations and radiometric equalization during the iterations showed slightly better results compared to the other matching versions. ATSR2 images were matched with a similar approach, however without geometric constraints, as the input images were rectified. Due to differences between the images which vary spatially, varying matching parameters are optimal for each image region. First steps in combining matching results from such varying matching versions have been performed. Both datasets showed similar matching problems due to surface discontinuities, mixing of surfaces than are neighbouring in image space but differ in height, and often large illumination differences (even with along-track stereo and small time acquisition differences).

1 INTRODUCTION

CLOUDMAP is a EU project for the detection and mapping of cirrus clouds and airplane contrails using satellite sensors for weather forecasting and climate change analysis. The scientific objectives of the project are to provide new cloud products (height, type, optical thickness, fraction etc.), compare different techniques for the extraction of some of these products (brightness temperature, stereoscopy and Oxygen A-band) and to validate them using airborne sensor underflights and ground-based remote sensing instruments. The requirements for cloud-top heights are very high temporal resolution, low geometric resolution, high processing speed and an accuracy of 100 to 500 m, depending on the application.

This paper will describe the results obtained in cloud-top height estimation from satellite sensors using stereo images at various resolutions (MOMS-2P and ATSR2) and spectral content (ATSR2). The exact knowledge of cloud-top heights is still a problem in satellite meteorology. The cloud heights derived from the radiation temperatures of infrared channel data include uncertainties mainly because many clouds are not blackbody sources, do not always fill the full pixel size and there is insufficient knowledge of the atmospheric temperature profiles. Photogrammetric methods based on stereoscopy are independent of these factors and are, therefore, useful for an improvement of cloud-height determinations. (Lorenz, 1985). Different authors (e.g. Hasler, 1991) have shown that cloud-height measurements made from stereoscopic satellite images can be used for a broad spectrum of meteorological processes.

2 CLOUD-TOP HEIGHT ESTIMATION FROM MOMS-2P

The MOMS stereopair (Fig. 1) was taken over South Germany on March 14th, 1997, from the MIR - Priroda mission, from a height of approximately 400 km. MOMS-02 is a three-line sensor (Ebner et al., 1996; Kornus, 1998), with along-

track stereo viewing, provided by a high resolution nadir-looking lens and two off-nadir lenses, forward (+21.4 degrees, channel 6) and backward (-21.4 degrees, channel 7) looking.

The two images used in this work were taken from channel 6 and channel 7, with a time delay of 40 seconds and a ground resolution of 18 m. The nadir image could not be used because channel 5 on Priroda was defocussed. Each image has a dimension of 2976 pixels across-track and 10472 pixels along-track and consists of a combination of two overlapping images in the flight direction. Clouds are generally visible, but they can not be always recognized in both images (Fig. 2) or they have different lightness and contrast (Fig. 1), because of the different illumination-to-sensor angle. Moreover, some other smaller structures (e.g. buildings) also appear different in the two images. The time difference between the two acquisitions causes some additional displacement and deformation of the clouds.

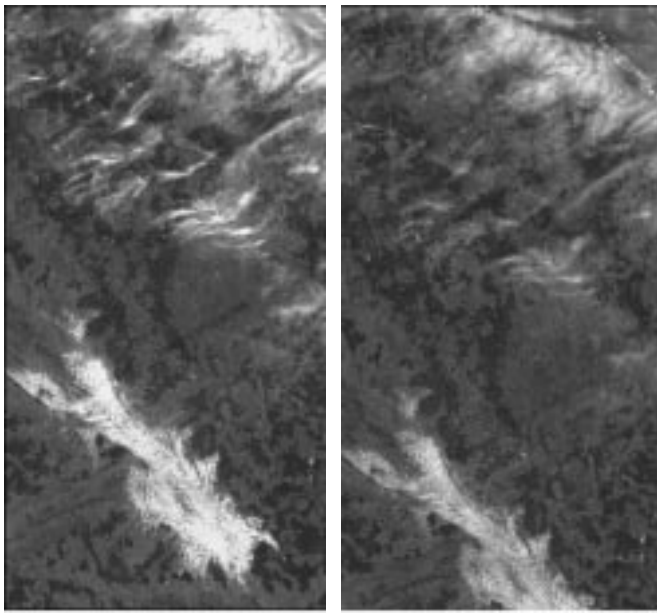

(a) (b)

Figure 1. MOMS-2P stereopair: channel 6 (a) and channel 7 (b).

The radiometric quality of the images was improved by reducing the noise and applying a Wallis filter (Wallis, 1976) for contrast enhancement and radiometric equalization. A further preprocessing was necessary to detect and reduce vertical stripes due to the saturation of the even columns in cloud regions. A 3x1 template window moves with step 2 in *x*-direction and step 1 in *y*-direction. If the grey mean value in the window is bigger than 230 and the correlation with a template containing typical stripes is bigger than 0.9, a filter is applied: the grey values are calculated again using a 5x1 mask. As a result, regions with vertical stripes became more homogeneous than before and some details appeared, as shown in Fig. 3.

(a)

(b)

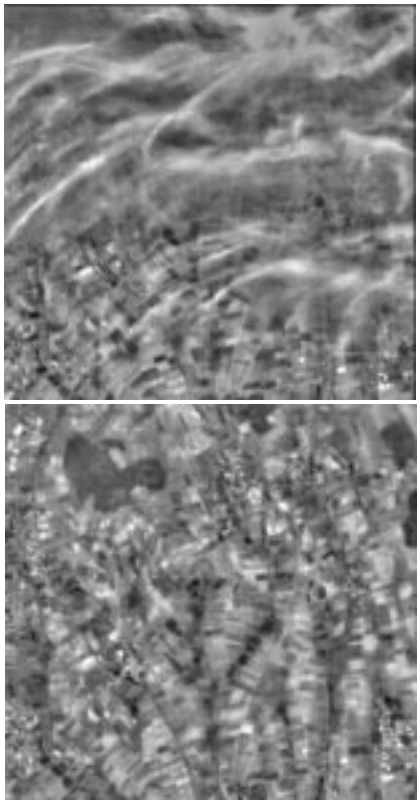

Figure 2. Example of cloud illumination differences, particularly with thin clouds, between channel 6 (a) and 7 (b).

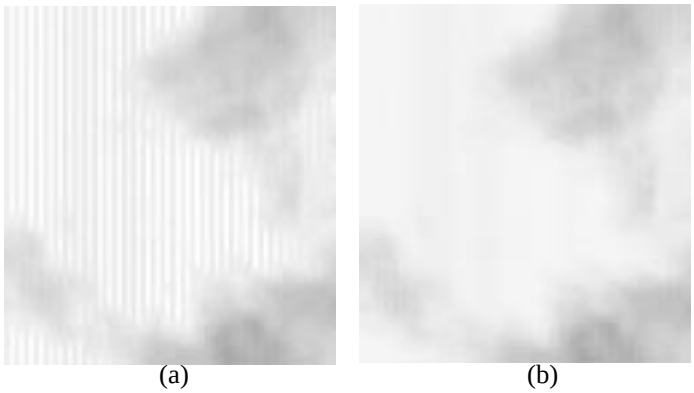

(a) (b)

Figure 3. Zoom in a saturated region before (a) and after (b) applying the filter.

Ground control points (GCPs) were acquired from a 1:50000 digital topographic map. 29 points were measured in the map, manually measured in the left image and transferred to the other one with semi-automatic least squares matching (Fig. 4). The program SPOTCHECK+ (version 3.2) developed by Kratky was used for the bundle adjustment. For a description of the model see Kratky (1989). The program was tested with different number of GCPs and with linear and quadratic functions to model the attitude changes, taking into account that the minimum number of needed full control points is 4 for the linear model and 6 for the quadratic one. Optimal results were obtained using 10 GCPs and quadratic attitude rates. In this case, the RMS errors of the remaining 19 check points were: 5.2 m in X, 4.4 m in Y and 11.1 m in Z. The strict sensor model was then approximated with polynomial mapping functions (PMFs), that describe direct projection equations from ground space to image space and vice versa and from one image space to the other. PMFs consist of 3rd-4th order polynomials with 11 - 16 terms, that are estimated with least square adjustment. The advantage of PMFs is that they are almost equally accurate as the strict model, but they are much faster. These functions will be further used to impose geometric constraints during the matching: they define quasi-epipolar lines along which the corresponding points are searched. The processing steps for MOMS sensor modelling and subsequent matching were similar to the ones described in Baltsavias and Stallmann (1996).

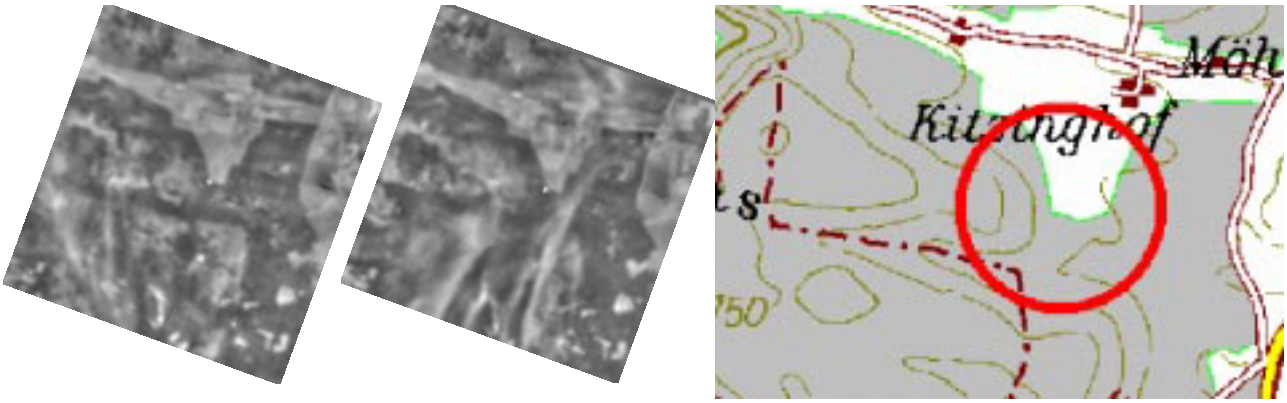

Figure 4. Identification of GCPs (white dot at image center) in the images and in the map.

For cloud-top heights, an accuracy from 100 to 500 m is required, thus coarse resolution images could suffice. Thus, we resampled the high resolution MOMS images to 288 m, estimated the cloud heights from these and the original images and compared the results, using the estimated heights from the original images as reference data. For matching, pyramid levels 6 to 4 were used (1152 to 288 m footprint), with the original images being level 0. An interest operator (Förstner and Gülch, 1987) was used to detect points on the fifth level of channel 6 that had better image quality. About 9000 interest points were found, projected on level 6 and matched with the PMFs. The points were then sequentially projected on levels 5 and 4 and matched with the help of the corresponding PMFs.

The algorithm for matching had to take into account the low texture of the clouds, the discontinuous, sometimes transparent or semi-transparent cloud form, and the cloud movement during the time interval between the acquisition of the images. These problems were reduced, by using least squares matching with the above mentioned geometric constraints (Baltsavias, 1991) and different geometric transformations for each level. On the highest level, shifts and a 7x7 pixel patch size and on the fifth level shifts and a rotation and a 9x9 patch size were used. On level 4, the matching algorithm was run in 6 versions, with three transformations (conformal/ rotations/ shifts) and with/without radiometric adjustment at each iteration. A quality analysis on the matching statistics and on the coordinates was made. At first, absolute and relative tests were applied on the matching statistics of each point (number of iterations, correlation coefficient, sigma 0 and shift/rotation/scale) to delete blunders, then points with height outside the known 350 - 8150 m range were deleted. Overall, about 25-30% of the points were rejected. The estimated ground coordinates were controlled by semi-automated, manually controlled least squares matching of 55 reference points (well defined and distributed) in order to choose the best matching configuration for level 4. The difference in the versions with/without radiometric adjustment was not large, with the first one being generally slightly better. Table 1 shows statistics of the height differences (mean with sign, maximum absolute, RMS) between reference data and the three matching versions of level 4 using radiometric adjustment at each iteration. The heights were compared before and after applying the two quality analysis tests. As Table 1 shows, although the tests improve the error statistics, many very big blunders, often in clusters, remain in the data, distort the error statistics and do not allow a comparison of the 3 geometric transformations used in matching. Thus, a last comparison was obtained by using the points after the two tests and after manually eliminating points with ΔZ bigger than 1100 m. For a base/height ratio of 0.77, an expected mean matching error of 1

pixel on level 4 would result to ca. 370 m height error, so we considered blunders (3 RMS) heights with errors larger than ca. 1100 m. The accuracy of the remaining match points is very high at ca. 0.2 pixels, showing the potential of our matching method, if large blunders can be excluded.

Transformation used in matching	Match point dataset used	# of match points	# of reference points	Mean	Max. Abs.	RMS
conformal	before tests	8891	55	1100	7189	2776
	after 2 tests (after 1st test) % rejected points	6148 (6643) 30% (25%)	42	904	7189	2313
	after 2 tests and blunder elim.	6148	36	41	203	74
rotations	before tests	8891	55	1162	6994	2786
	after 2 tests (after 1st test) % rejected points	6539 (7366) 26% (17%)	43	886	6994	2304
	after 2 tests and blunder elim.	6539	37	35	154	66
shifts	before tests	8891	55	1168	7006	2798
	after 2 tests (after 1st test) % rejected points	6636 (7731) 25% (13%)	45	986	7006	2427
	after 2 tests and blunder elim.	6636	38	38	210	69

Table 1. Statistics of height differences (in m) between semi-automatic measurements in the original images and automatic matching in low resolution images (288 m). The matching in the low resolution images was provided using different transformations (conformal, rotation, shifts) and radiometric adjustment in every iteration. Two automated tests to detect blunders were applied. Blunder elimination was manual to show the accuracy potential of matching.

After comparing the results, we chose as best version the one obtained with rotations. Contour lines with a interval of 200 m were interpolated, and overlapped on a high resolution image. Two groups of clouds at different height were identified: the group in the top of the image, with a top height of 4000-7400 m, and the group in the bottom, which is very low (down to 600 m). Fig. 5 shows contour lines (for Z >1000 m) of the region containing the group of high cirrus clouds and the same region in the original image. This figure demonstrates nicely some of the matching problems encountered. Using area-based matching, land areas between the clouds and close to their borders, are attracted during matching due to the bright higher-contract clouds to a totally wrong height, i.e. those of the clouds. These land points can not be recovered during matching in lower pyramid levels as they are very far away from the correct points. Furthermore, since they were within the acceptable height range and they had stuck to a side minimum, they could not detected by the two quality tests applied. These problems are nicely shown in the contours of the lower middle part (Fig. 5), where land points are lifted up at the cloud-top heights, whereas in the upper middle part, where large land areas with no clouds exist, points are correctly matched. Another disadvantage of area-based matching is that it does not allow a good modelling of cloud borders, leading to smoothing. These effects become worse, the higher the pyramid level is, so feature-based matching and/or starting from lower pyramid levels will lead to reduction of these problems. Additional matching problems were caused for this stereopair, due to the large parallax (height) range. To start of 1-2 pixels approximations, a pyramid level higher than the 6th one would be needed, but then the image would become extremely small. Thus, we started from level 6th living with the fact that some points could never be correct due to poor approximations.

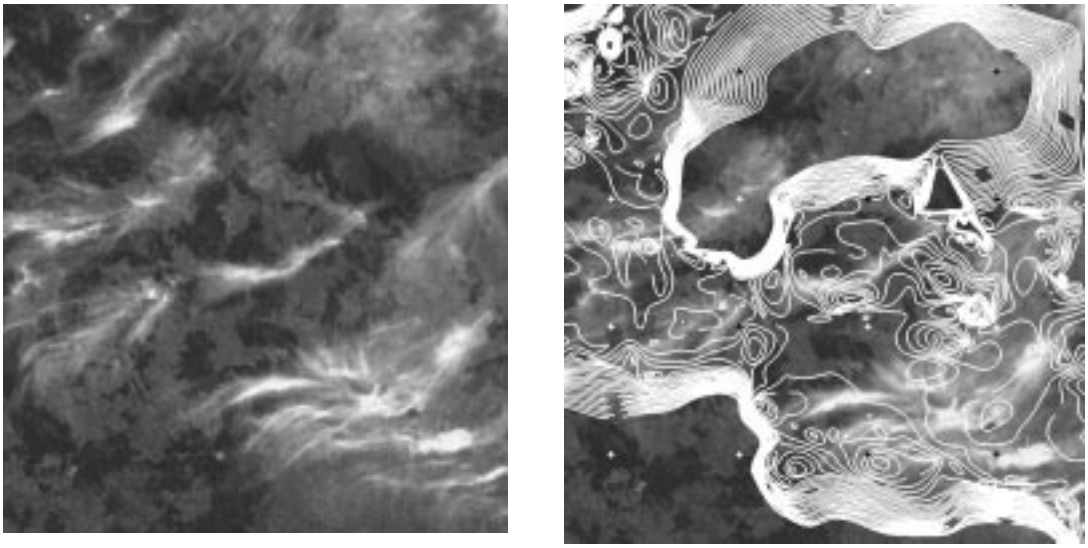

Figure 5. Contour lines with 200 m interval (right) in a region covered by cirrus clouds (left).

3 CLOUD-TOP HEIGHT ESTIMATION FROM ATSR2

The ATSR2 data were collected from the ESA ATSR NRT service (Buongiorno, 1999) during the Special Observation Period (SOP) of the programme MAP (Mesoscale Alpine Programme). MAP is an international research initiative devoted to the study of atmospheric and hydrological processes over mountainous terrain (MAP Science Plan, 1998). The SOP period lasted from September, 7 to November, 15, 1999 and was concentrated to three target areas in the inner Alpine region of Italy, Switzerland and Austria.

The ATSR2 instrument is part of the ERS-2 satellite system which was launched in April 1995. The successor sensor, AATSR, will be part of Envisat which is currently scheduled for June 2001. ERS-2 is in a near-circular, sun-synchronous orbit at a mean height of 780km and a sub-satellite velocity of 6.7 kms^{-1}. The spacecraft is positioned to operate with a descending equator crossing of around 10:30 local solar time and of a ascending equator crossing of 22:30 local solar time. The repeat cycle is about 3 days. First, the ATSR2 views the surface along the direction of the orbit track at an incidence angle of 55˚ as it flies toward the scene. Then, some 120s later, ATSR2 records a second observation of the scene at an angle close to the nadir (Mutlow, 1999). ATSR2's field of view comprises two 500 km-wide curved swaths, with 555 pixels across the nadir swath and 371 pixels across the forward swath. The pixel size is 1x1 km at the center of the nadir scan and 1.5 x 2 km at the center of the forward scan. The sensor records in 7 spectral channels: 0.55µm, 0.67µm, 0.87µm, 1.6µm, 3.7µm, 10.8µm, 12.0µm. The geolocation for the GBT products proceeds by mapping the acquired pixels onto a 512x512 grid with 1km pixel size whose axes are the ERS-2 satellite ground-track and great circles orthogonal to the ground-track. The resampling is done using a nearest neighbor method (Mutlow, 1999).

Several significant data quality problems can be found in the delivered ATSR2 images which are also reported in (Danson et al., 1999):

- Differences of odd/ even pixels: Fig. 5 shows a part of an enhanced ATSR2 nadir image from the 0.87µm channel. The difference between odd and even pixels is obvious. The reason is that odd and even pixels from the sensor are calibrated separately as they are obtained from different integrators (Mutlow, 1999 and personal communication).
- Scan jitter: Correct positional registration of the 2000 pixels around a scan relies on a steady scan rotation rate. A scan jitter arises when the rotation speed of the scan mirror deviates from this, as can happen if the rotation is obstructed by debris. Irregular rotation results in a misalignment of data from successive scans (Mutlow, 1999).
- Nearest neighbor resampling: due to this resampling method which is used to generate the GBT data, a sort of "stairs" is introduced in the images (Fig. 6).

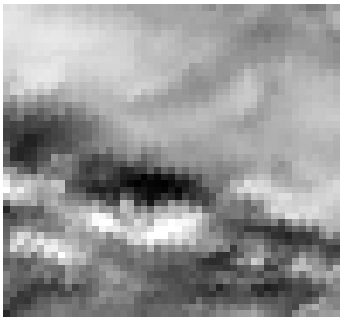

Figure 6. Difference between odd and even columns.

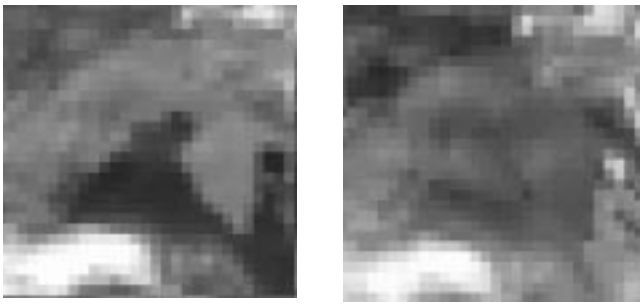

Figure 7. Differences between nadir image (left) and forward image (right). Northern Adria.

The ATSR2 GBT data were reduced to 8-bit and linearly stretched between the minimum and maximum value, cutting 0.5% on both sides of the histogram (excluding the pixels assigned with an error code). To reduce the image quality problems (Fig. 6), a 3x3 median filter has been used before the generation of the image pyramid. As no a priori values of the cloud heights are given to the matching algorithm, a hierarchical matching procedure with 3 pyramid levels is applied so that the maximum possible parallax at the highest level is only 1-2 pixels. Every pyramid level is enhanced and radiometrically equalized with a Wallis filter. 44919 points are selected with an interest operator in the first pyramid level because it is likely that the same points are well detectable also in the third level and the original image.

The matching was done with the unconstrained mode of the Multi-Photo Geometrically Constrained Matching Software package developed at our institute (Baltsavias, 1991), which is based on Least-Squares-Matching (Grün, 1985). Two independent results were processed through all pyramid levels, one working on the grey-level image, one working on the derivative image. For both sets, a 3x3 mean filter was included in the matching of the original image to smooth closed regions introduced by the previously applied median filter.

Due to the different looking angle and the not equal pixel size of the two images, matching can be very difficult, especially with thin differently looking clouds (Fig. 7). It is also necessary to work with different matching parameters as every version can be good for some areas but unsuccessful in other regions. Fig. 7 shows the Northern Adria region where the second method (derivative image) could solve the problem of the strong illumination difference between nadir and forward image (see also Fig. 8).

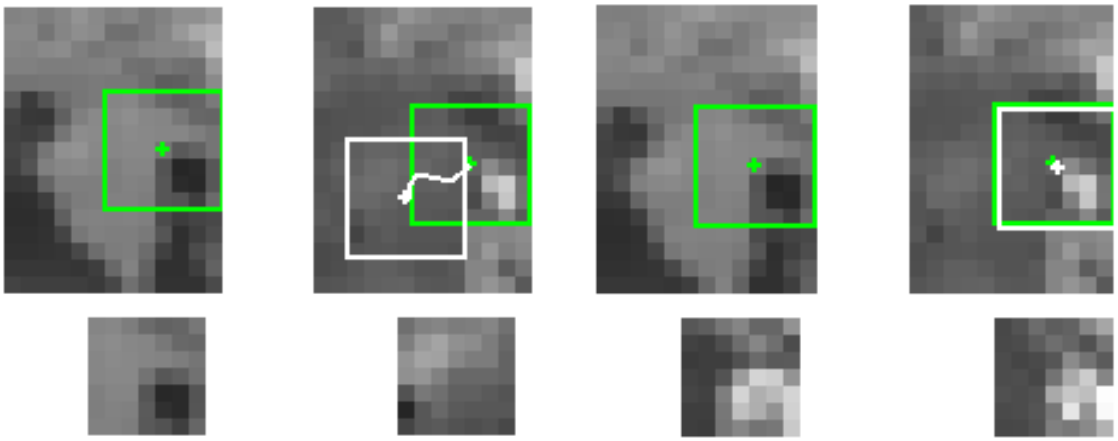

Figure 8. Left: unsuccessful matching on grey-level image, right: successful matching on derivative image.

The solutions of the two sets are first independently quality-controlled with absolute tests on the x- and y-disparities and relative tests on the correlation coefficient, sigma 0 and the change from the approximations in x- and y-direction. Afterwards, the two sets are combined in the following way: points which just exist in one version after the quality control are taken without further examination. For the other points, the x- and y-disparities, sigma 0 and the correlation coefficient is compared to decide which point version is taken.

The resulting y-parallaxes are a function of the height, the along-track wind component (only for clouds) and of the nadir and forward zenith angle. The nadir and forward zenith angle are known at 11 equally distributed points of the first and last scan line from the GBT header and can be linearly interpolated for all pixels (Bailey, 1995). If no cloud motion information is available, the cloud height h is calculated from the uncorrected y-parallax y_p after (Prata and Turner, 1997):

$$h = \frac{y_p}{\tan((\chi_f) - \tan(\chi_n))} \quad (1)$$

where x_f, x_n forward/nadir zenith angle
y_p: parallax in y-direction

If either the cloud wind vector or the total cloud wind velocity is available from another source (e.g. Meteosat cloud winds), the y-parallax can be corrected for the wind-induced along-track amount. The x-parallax is a function of the across-track wind component and of the resampling error (for gridded products). For the wind corrections, the exact time difference between the same pixel in the forward and the nadir scan has to be calculated from the along-track distance and the satellite velocity.

4 CONCLUSIONS

The potential of deriving cloud-top heights from stereo satellite images with 288 m and 1000 m resolution has been demonstrated. The same algorithms could be used with both datasets. Preprocessing and post-processing blunder detection algorithms led to improvements. The accuracy potential of our matching approach, as shown with the MOMS data, is well into the subpixel range, being able to fulfil the accuracy requirements for applications in weather and climate. Similar matching problems were encountered, with slightly more for MOMS due to the larger parallax range and higher resolution. Large blunders remain undetected in the results, caused mainly by the surface discontinuities, mixing of image neighboring areas of large vertical separation, reflectance differences, and poor approximate values. Approaches to reduce these problems have been already identified and will be implemented in future investigations.

ACKNOWLEDGEMENTS

We would like to thank Dirk Stallmann, Institute for Photogrammetry, University of Stuttgart for providing valuable help in processing of the MOMS-02 imagery and Chris Mutlow, Rutherfold Appleton Laboratory, for valuable comments about the ATSR2 data. The ATSR2 data was kindly provided by the ESA NRT service.
This work is funded by the Bundesamt für Bildung und Wissenschaft (BBW) within the EU-project CLOUDMAP (BBW Nr. 97.0370).

REFERENCES

Bailey, P., 1995. SADIST-2 v100 products. ER-TN-RAL-AT-2164, Rutherford Appleton Laboratory.

Baltsavias, E.P., 1991. Multiphoto geometrically constrained matching. Ph. D. dissertation, Institute of Geodesy and Photogrammetry, ETH Zürich, Mitteilungen No. 49, 221 p.

Baltsavias, E. P., Stallmann, D., 1996. Geometrical potential of MOMS-02/P data for point positioning, DTM and orthoimage generation. IAPRS, Vol. 31, Part B4, pp. 110 - 116.

Buongiorno, A., 1999. WWW ATSR Near Real Time service, quick guide, version 1.0. ESA/ ESRIN.

Danson, F.M., Higgins, N.A., Trodd, N.M., 1999. Measuring land-surface directional reflectance with the along-track scanning radiometer. Photogrammetric Engineering and Remote Sensing, 65 (12), pp. 1411-1417.

Ebner, H, Ohlhof, T., Putz, E., 1996. Orientation of MOMS-02/D2 and MOMS-2P imagery. IAPRS, Vol. 31, Part B3, pp. 158-164.

Förstner, W., Gülch, E., 1987. A fast operator for detection and precise location of distinct points, corners, and centers of circular features. Proc. ISPRS Intercommission Conf. on Fast Processing of Photogrammetric Data, Interlaken, Switzerland, 2-4 June, pp. 281-305.

Grün, A., 1985. Adaptive least squares correlation: a powerful image matching technique. S. Afr. J. of Photogrammetry, Remote Sensing and Cartography, 14 (3), pp. 175-187.

Hasler, F., 1991. Automatic analysis of stereoscopic satellite image pairs for determination of cloud-top height and structure. J. Appl. Met., 30 (3), pp. 257-281.

Kornus, W., 1998. Dreidimensionale Objektrekonstruktion mit digitalen Dreizeilenscannerdaten des Wetraumprojekts MOMS-02/D2. Forschungsbericht 97-54, Oberpfaffenhofen, Germany.

Kratky, V., 1989. Rigorous photogrammetric processing of SPOT images at CCM Canada. ISPRS Journal of Photogrammetry and Remote Sensing, Vol. 44, pp. 53-71.

Lorenz, D., 1985. On the feasibility of cloud stereoscopy and wind determination with the along-track scanning radiometer. Int. J. Rem. Sens., 6 (8), pp. 1445-1461.

MAP Science Plan, 1998. http://www.map.ethz.ch/span/spindex.htm (accessed April 2, 2000).

Mutlow, Ch., 1999. ATSR-1/2 User Guide, Issue 1.0, Rutherford Appleton Laboratory.

Prata, A.J., Turner, P.J., 1997. Cloud-top height determination using ATSR data. Rem. Sens. Env., 59, pp. 1-13.

Wallis, R., 1976. An approach to the space variant restoration and enhancement of images. Proc. of Symposium on Current Mathematical Problems in Image Science, Naval Postgraduate School, Monterey, California, USA.